# Structure of a Myristoyl-ACP-Specific Thioesterase from *Vibrio harveyi*†

D. M. Lawson,‡,§ U. Derewenda,‡ L. Serre,‡ S. Ferri,‖ R. Szittner,‖ Y. Wei,‡ E. A. Meighen,*,‖ and Z. S. Derewenda*,‡

*Medical Research Council of Canada Group in Protein Structure and Function, Department of Biochemistry, University of Alberta, Edmonton, Alberta, T6G 2H7 Canada, and Department of Biochemistry, McGill University, Montreal, Quebec, H3G 1Y6 Canada*

*Received April 20, 1994; Revised Manuscript Received May 27, 1994*®

ABSTRACT: The crystal structure of a myristoyl acyl carrier protein specific thioesterase ($C_{14}$ACP-TE) from a bioluminescent bacterium, *Vibrio harveyi*, was solved by multiple isomorphous replacement methods and refined to an *R* factor of 22% at 2.1-Å resolution. This is the first elucidation of a three-dimensional structure of a thioesterase. The overall tertiary architecture of the enzyme resembles closely the consensus fold of the rapidly expanding superfamily of $\alpha/\beta$ hydrolases, although there is no detectable homology with any of its members at the amino acid sequence level. Particularly striking similarity exists between the $C_{14}$ACP-TE structure and that of haloalkane dehalogenase from *Xanthobacter autotrophicus*. Contrary to the conclusions of earlier studies [Ferri, S. R., & Meighen, E. A (1991) *J. Biol. Chem. 266*, 12852–12857] which implicated Ser77 in catalysis, the crystal structure of $C_{14}$ACP-TE reveals a lipase-like catalytic triad made up of Ser114, His241, and Asp211. Surprisingly, the $\gamma$-turn with Ser114 in a strained secondary conformation ($\phi = 53°$, $\psi = -127°$), characteristic of the so-called nucleophilic elbow, does not conform to the frequently invoked lipase/esterase consensus sequence (Gly-X-Ser-X-Gly), as the positions of both glycines are occupied by larger amino acids. Site-directed mutagenesis and radioactive labeling support the catalytic function of Ser114. Crystallographic analysis of the Ser77 → Gly mutant at 2.5-Å resolution revealed no structural changes; in both cases the loop containing the residue in position 77 is disordered. The oxyanion hole does not appear to be fully formed in the native enzyme, suggesting that its structural reorganization may occur upon substrate binding, a mechanism reminiscent of the conformational changes underlying interfacial activation in triglyceride lipases.

Thioesterases are ubiquitous hydrolytic enzymes involved in many biochemical phenomena, including the biosynthesis of fatty acids (Libertini & Smith, 1978; Lin & Smith, 1978; De Renobales *et al.*, 1980; Voelker *et al.*, 1992) and biologically active polyketides, such as immunosuppressants, cancer agents, and peptide antibiotics (Donadio *et al.*, 1991; Shen & Hutchinson, 1993; McDaniel *et al.*, 1993; Kratzschmar *et al.*, 1989; Raibaud *et al.*, 1991), in bioluminescence (Ferri & Meighen, 1991), in regulation of intracellular fatty acids and acyl-CoA[1] derivatives (Sanjanwala *et al.*, 1987), and in the removal of palmitoyl groups from posttranslationally acylated Ras proteins (Camp & Hofmann, 1993). Although they constitute a key subclass of hydrolases, to date no three-dimensional structure has been reported for any of these enzymes.

In light-emitting bacteria (including *Vibrio harveyi*), a specific thioesterase is responsible for the cleavage of the tetradecanoyl (myristoyl) acyl chain from the acyl carrier protein (ACP) of the fatty acid synthase (FAS) complex and for diverting it to the bioluminescence pathway (Ferri & Meighen, 1991), where it undergoes NADPH-dependent reduction and subsequent $FMNH_2$- and $O_2$-dependent oxidation of the corresponding aldehyde, with accompanying emission of light. The enzyme is capable of transferring the acyl group from acyl-ACP and acyl-CoA to glycerol, ethylene glycol, and $\beta$-mercaptoethanol (Carey *et al.*, 1984), and it hydrolyzes myristoyl oxyesters (Ferri & Meighen, 1994). Hence, it was described in the past as both an acyltransferase and an esterase, although it should be classified on the basis of its primary function *in vivo* as a myristoyl-ACP thioesterase ($C_{14}$ACP-TE).

The *V. harveyi* TE is a 32-kDa polypeptide chain with 305 amino acids. It is inactivated by phenylmethanesulfonyl fluoride, and neutral hydroxylamine has no effect on the acyl-enzyme intermediate; furthermore, a group with a $pK_a$ of 6.3 was found to play a key role in catalysis (Ferri & Meighen, 1991). These results strongly suggested that a seryl residue and a histidyl residue are present in the active site. The DNA-deduced amino acid sequence (Ferri & Meighen, 1991) was subsequently shown to contain the pentapeptide Gly-Leu-Ser-Ser-Gly, consistent with the so-called lipase/esterase consensus motif Gly-X-Ser-X-Gly (Brenner, 1988), suggesting that Ser77, located at the center of this motif, is the active nucleophile within a possible Ser-His-(Asp/Glu) catalytic triad. The presence of similar triads—reminiscent of, but in details different from, those found in the chymotrypsin and subtilisin families of serine proteinases—has been found in a number of hydrolases degrading oxy–ester bonds, including lipases (Brady *et al.*, 1990; Winkler *et al.*, 1990; Schrag *et al.*, 1991; Noble *et al.*, 1993), cutinase (Martinez *et al.*, 1992),

† Research supported by the Alberta Heart and Stroke Foundation (Z.S.D.), the MRC of Canada, grants to the Group in Protein Structure and Function (Z.S.D.) and MT-4314 (E.A.M.), and the Alberta Heritage Foundation for Medical Research (Z.S.D.). D.M.L. was supported by Novo-Nordisk Industri A/S. Z.S.D. is a Medical Scholar of the AHFMR.

* Authors to whom correspondence should be addressed.

‡ University of Alberta.

§ Permanent address: Department of Chemistry, University of York, Heslington, York Y01 5DD, U.K.

‖ McGill University.

® Abstract published in *Advance ACS Abstracts,* July 1, 1994.

[1] Abbreviations: $C_{14}$ACP-TE, myristoyl acyl carrier protein thioesterase from *Vibrio harveyi*; TE, thioesterase; CoA, coenzyme A; ACP, acyl carrier protein; FAS, fatty acid synthase; SIRAS, single isomorphous replacement anomalous scattering; MIR, multiple isomorphous replacement; Hal, haloalkane dehalogenase from *Xanthobacter autotrophicus*.

0006-2960/94/0433-9382$04.50/0 

and acetylcholinesterase (Sussman *et al.*, 1991). The proposed structure of the active site was also consistent with the fact that substitutions in position 77 (Ser → Ala, Thr, Gly) inactivate the enzyme (Ferri & Meighen, 1991).

In this paper we report an initial description of the three-dimensional fold and active site geometry of the enzyme and reassess the catalytic mechanism of $C_{14}$ACP-TE in the light of the crystal structure. A complete description of all the details of the molecular structure of the enzyme will be reported upon completion of high-resolution refinement based on synchrotron X-ray data.

## MATERIALS AND METHODS

*Wild-Type Enzyme Crystallization.* The enzyme was overexpressed, purified, and crystallized as described elsewhere (Swenson *et al.*, 1992). The crystals were monoclinic (space group $P2_1$, $a$ = 89.9 Å, $b$ = 83.6 Å, $c$ = 47.1 Å, $\beta$ = 97.3°) with two molecules in the asymmetric unit related by a pronounced noncrystallographic diad and a solvent content of approximately 50%.

*Structure Solution.* All four heavy atom derivatives used in structure solution were prepared by soaking native crystals under the following conditions: Hg derivative, 10 mM $HgCl_2$ for 4 days; Pt, 1 mM chloro(2,2′:6′,2″-terpyridine)platinum-(II) chloride for 2 days; I, 3 mM *N*-iodosuccinimide anhydride for 12 h; U, 10 mM uranyl acetate for 5 days. X-ray data were collected on Xentronics (Siemens) area detectors mounted on rotating anode generators (Rigaku RU200 in York and Siemens in Edmonton) equipped with graphite monochromators. The native and iodo derivative data were processed using XENGEN (Howard *et al.*, 1987); the remaining data sets were processed using XDS (Kabsch, 1987). Relevant crystallographic details are presented in Table 1. All subsequent calculations were carried out using the CCP4 suite for protein crystallography (SERC Daresbury Laboratory, Daresbury, U.K.), unless stated otherwise. Eight Hg sites were located using Patterson search techniques and used to calculate SIRAS phases; the latter were used in difference Fourier calculations which revealed the heavy atom positions in other derivatives. Three sites were common to the I and U derivatives; one of these was also found in the Pt derivative. The refinement of all heavy atom positions and calculation of phases were carried out using MLPHARE (CCP4). The solvent flattening procedure using SQUASH (Zhang, 1993) produced an electron density map which clearly defined the molecular envelopes but failed to reveal adequate detail for model building. The noncrystallographic symmetry was precisely determined using the symmetry-related heavy atom sites in the Hg and Pt derivatives. Noncrystallographic map averaging (Jones *et al.*, 1991) was followed by inverse Fourier transform, and the resulting phases were combined with the MIR phases. These combined phases were used in SQUASH in the second cycle of solvent flattening followed by phase extension to 2.5 Å. At this point an electron density map, calculated at 2.5-Å resolution and averaged around the noncrystallographic 2-fold axis, was sufficiently interpretable to build approximately 70% of the amino acids. The partial structure was refined using XPLOR (Brunger, 1988), and the calculated phases were once more combined with the MIR phases. This last map allowed most of the remaining amino acids to be modeled into electron density.

*Refinement.* Least squares crystallographic refinement was carried out using all data within the resolution range 8.0–2.06 Å by iterative rounds of restrained and unrestrained refinement using XPLOR (Brunger, 1988), PROLSQ (CCP4), and ARP (Lamzin & Wilson, 1993), with intervening manual revisions of the structure using O (Jones *et al.*, 1991) on an SGI Indigo² Extreme system. The final set of coordinates was obtained after XPLOR with both positional and thermal parameters refined. The temperature ($B$) factors were restrained so that the $\sigma$ value for 1–2 bonded atoms (covalent bonds) was set to 1.5 Å², while the 1–3 (angle) was 2.0 Å².

*Site-Specific Mutagenesis and Radioactive Labeling.* Mutagenesis of Ser77 and Ser114 was done using the M13mp18 vector and synthetic primers GTGGGGCTCGGCTCGGGTTCG and GATTGCGGCAGGTCTCTCAGCT to convert the respective serine residues to glycines (Kunkel *et al.*, 1987; Tabor & Richardson, 1985). The *Escherichia coli* K38 cells containing the pGP1-2 plasmid coding for the T7 RNA polymerase and the pT7 recombinant plasmid with luxD were grown in LB medium containing 100

Table 1: Data Collection and Phasing Statistics[a]

| | Data Collection wild type | S77G mutant |
|---|---|---|
| X-ray data collection | | |
| nominal resolution (Å) | 2.06 | 2.46 |
| unique reflections | 36778 | 22900 |
| overall completeness (%) | 86.0 | 74.0 |
| inner shell | 94.3 (20.0–2.19 Å) | 99.2 (20.0–2.61 Å) |
| outer shell | 43.7 (2.19–2.06 Å) | 36.9 (2.61–2.46 Å) |
| $\langle I/\sigma(I)\rangle$ | 14.3 | 16.6 |
| outer shell | 1.35 (2.19–2.06 Å) | 1.11 (2.61–2.46 Å) |
| redundancy | 2.4 | 3.2 |
| $R_{merge}$ | 0.09 | 0.11 |

| Multiple Isomorphous Replacement Phasing | Hg | Pt | I | U |
|---|---|---|---|---|
| X-ray data collection | | | | |
| resolution (Å) | 3.4 | 3.4 | 3.4 | 3.4 |
| $R_{merge}$ | 0.08 | 0.08 | 0.09 | 0.06 |
| unique reflections | 8900 | 9102 | 7721 | 8928 |
| % complete | 94.9 | 97.0 | 82.3 | 95.2 |
| redundancy | 4.2 | 4.4 | 4.3 | 3.9 |
| no. of sites (major/minor) | 8/0 | 8/0 | 1/5 | 1/8 |
| $R_{iso}$ | 0.27 | 0.22 | 0.15 | 0.09 |
| overall phasing results | | | | |
| $R_{Cullis}$ acentric | 0.80 | 0.71 | 0.90 | 0.89 |
| $R_{Cullis}$ centric | 0.76 | 0.85 | 0.90 | 0.90 |
| phasing power acentric | 1.3 | 1.8 | 0.9 | 1.1 |
| phasing power centric | 1.0 | 1.2 | 0.6 | 0.8 |
| figure of merit $\langle m\rangle$ acentric | | | 0.59 | |
| figure of merit $\langle m\rangle$ centric | | | 0.75 | |

| phasing power in resolution shells | | | | | | | | |
|---|---|---|---|---|---|---|---|---|
| resolution (Å) | 8.10 | 6.74 | 5.77 | 5.06 | 4.51 | 4.08 | 3.70 | 3.40 |
| Hg acentric | 1.6 | 1.7 | 1.7 | 1.7 | 1.2 | 1.1 | 1.2 | 1.1 |
| Hg centric | 1.4 | 1.2 | 1.5 | 1.4 | 0.7 | 0.7 | 0.9 | |
| Pt acentric | 1.7 | 1.9 | 2.2 | 2.0 | 1.8 | 1.7 | 1.6 | 1.8 |
| Pt centric | 1.2 | 1.0 | 1.3 | 1.3 | 1.0 | 1.2 | 1.3 | 0.5 |
| I acentric | 1.0 | 1.2 | 1.3 | 1.2 | 1.0 | 0.8 | 0.8 | 0.7 |
| I centric | 0.8 | 0.4 | 0.8 | 0.6 | 0.7 | 0.6 | 0.6 | 0.5 |
| U acentric | 1.3 | 1.5 | 1.6 | 1.4 | 1.1 | 1.0 | 0.9 | 1.1 |
| U centric | 0.8 | 0.7 | 1.1 | 1.0 | 0.9 | 0.7 | 0.6 | |
| figure of merit in resolution shells | | | | | | | | |
| resolution (Å) | 8.10 | 6.74 | 5.77 | 5.06 | 4.51 | 4.08 | 3.70 | 3.40 |
| acentric | 0.67 | 0.68 | 0.68 | 0.66 | 0.61 | 0.58 | 0.55 | 0.51 |
| centric | 0.84 | 0.80 | 0.78 | 0.81 | 0.73 | 0.77 | 0.70 | 0.48 |

[a] The various crystallographic parameters are defined as follows: $R = \Sigma|F_o - F_c|/\Sigma|F_o|$, where $F_o$ and $F_c$ represent respectively the observed and calculated structure factors of the $i$th reflection, and the summation extends over all data; $R_{merge} = \Sigma|I_i - \langle I\rangle|/\Sigma I_i$, where $I_i$ is the intensity of the $i$th observation and $\langle I\rangle$ is the mean intensity of the reflection; $R_{iso} = \Sigma|F_{PH} - F_P|/\Sigma|F_P|$, the mean relative isomorphous difference between the native protein ($F_P$) and derivative ($F_{PH}$) data; $R_{Cullis} = \Sigma||F_{PH} + F_P| - F_H|/\Sigma|F_{PH} - F_P|$, where $F_H$ is the calculated heavy atom structure factor contribution; phasing power = $\langle F_H\rangle/\langle E\rangle$, where $\langle E\rangle$ is the rms lack of closure.

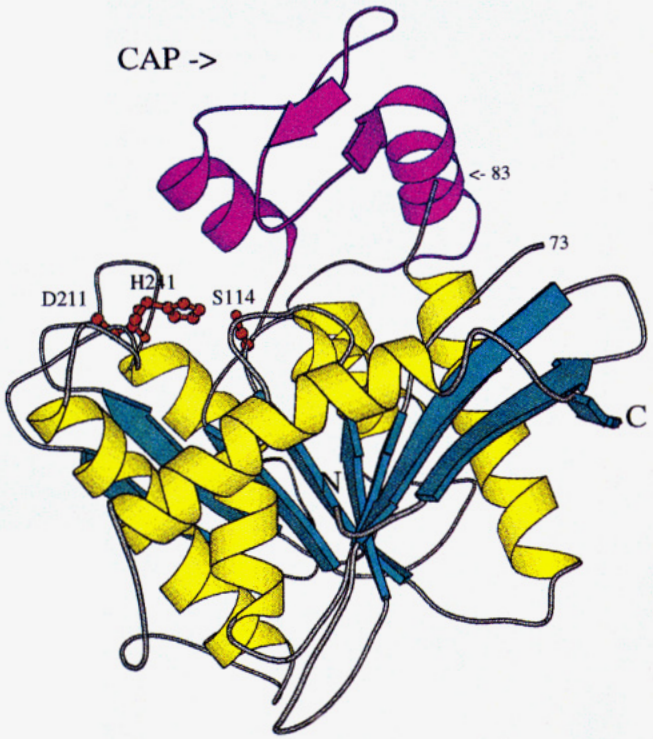


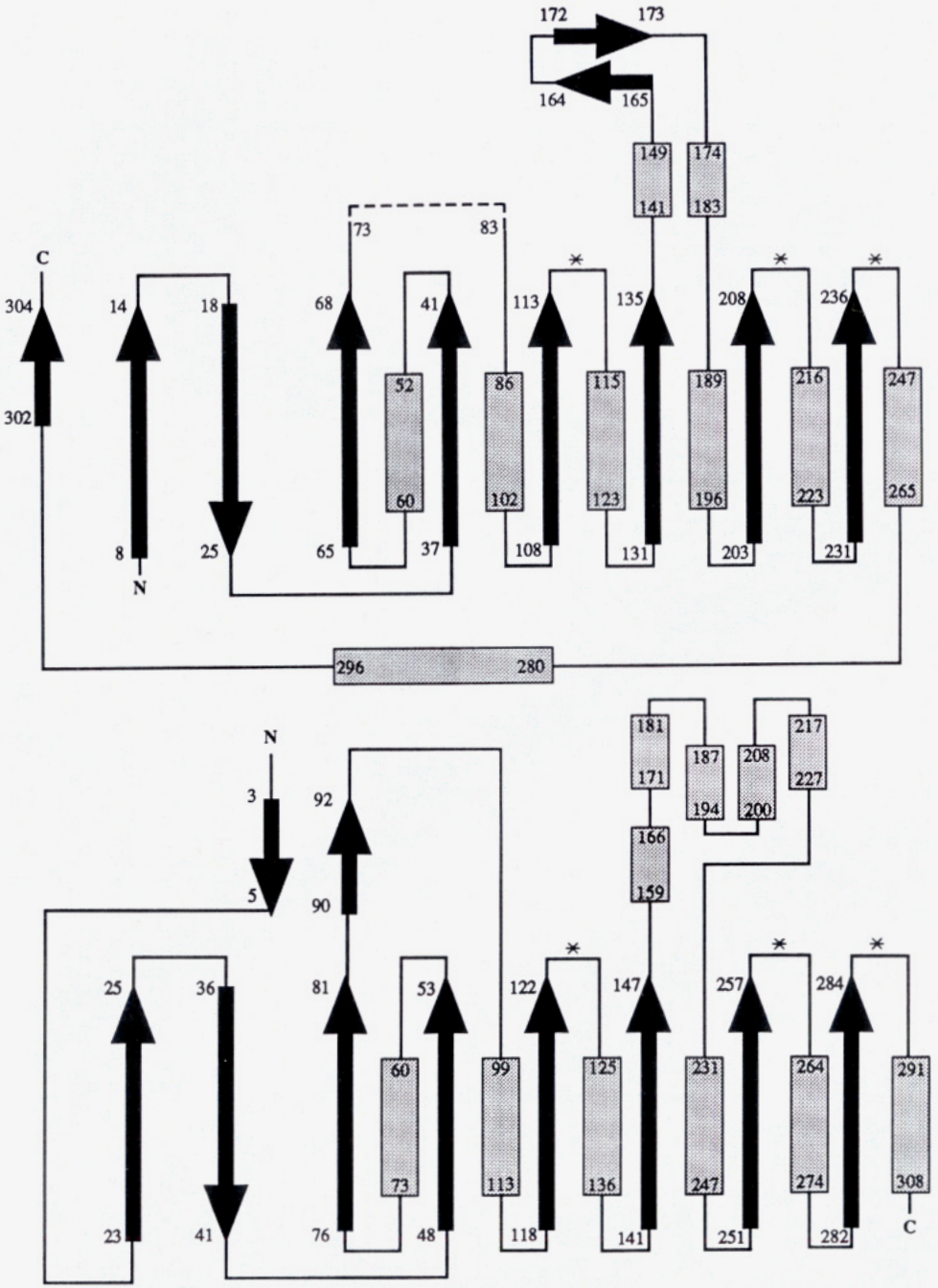


FIGURE 1: (a, left) Schematic representation of the three-dimensional structure of the molecule of the *V. harveyi* thioesterase. The "cap" subdomain is shown in pink; $\alpha$-helices and $\beta$-strands of the main domain are shown in yellow and blue, respectively. The catalytic triad is shown in full in red, and the amino and carboxyl termini are denoted by the letters N and C. Residues 73 and 83 which flank the surface loop invisible in the electron density map are indicated. The figure was generated using MOLSCRIPT (Kraulis, 1991). (b, c) Topologies of the *V. harveyi* $C_{14}$ACP-TE (b, top right) and haloalkane dehalogenase (Hal) (c, bottom right). The secondary structure analysis of the TE was carried out using DSSP (Kabsch & Sander, 1983); those for Hal were given by Verschueren *et al.* (1993a). The topology of the eight consecutive strands of the $\beta$-sheet can be described as $+1, +2, -1x, +2x, (+1x)_3$ (Richardson, 1981; Ollis *et al.*, 1992). The asterisks denote the positions of the catalytic residues which occur in the order Ser, Asp, His (Asp, Asp, His in Hal) along the polypeptide chain.

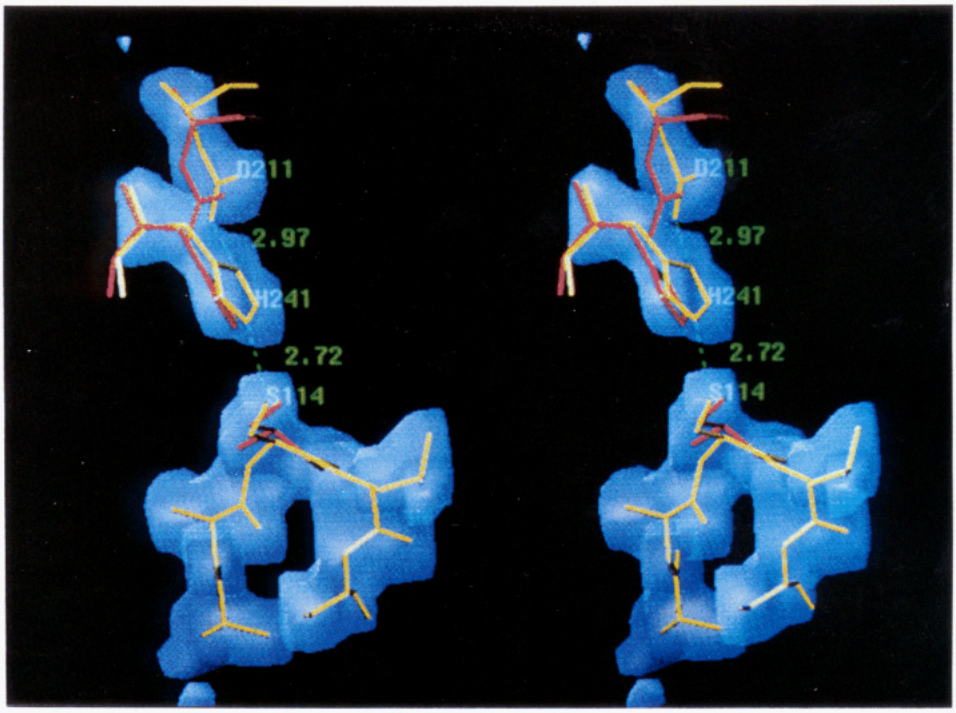


FIGURE 2: Catalytic triad of the *V. harveyi* thioesterase and its comparison with that observed in the *R. miehei* lipase. Difference electron density is shown for residues Ala112–Ser116, His241, and Asp211; it was calculated with coefficients $F_o - F_c$ after all seven residues were excluded from the model and the structure was subjected to additional cycles of refinement [XPLOR (Brunger, 1988)] to remove any bias in the phases; the map is contoured at a level of $3\sigma$. The hydrogen bonds within the catalytic triad are indicated together with interatomic distances; the catalytic triad of the *R. miehei* lipase is shown in red. The figure was generated using O (Jones *et al.*, 1991).

$\mu$g/mL ampicillin and 40 $\mu$g/mL kanamycin at 30 °C until $A_{660} = 0.5$, at which point the culture was transferred to a 42 °C shaking water bath for 25 min. The cultures were incubated with shaking for 2 h at 27 °C. Specific labeling with [$^{35}$S]methionine demonstrated that both mutants were expressed to similar levels in extracts. Cell extracts were obtained by sonification in 50 mM phosphate. The clarified extract was mixed with either 1 or 10 $\mu$M [$^{3}$H]myristoyl-CoA (18 Ci/mmol) for 30 s before being mixed with an equal volume of SDS–PAGE sample buffer and electrophoresis.

*X-ray Structure Determination of the Ser77 → Gly Mutant.* The site-specific mutant Ser77 → Gly was overexpressed and purified in a manner identical to that of the wild-type enzyme. The crystals grew easily within the range of conditions established for the wild-type protein and were fully isomorphous with those of the latter. Data were collected using the Siemens area detector mounted on a Siemens rotating anode generator, as described above. Details of data collection are given in Table 1. The atomic model obtained for the wild-type protein was refined using XPLOR against the diffraction data collected from the mutant, and an electron density map was calculated, displayed, and analyzed as described above.

## RESULTS

The refined atomic model of $C_{14}$ACP-TE consists of two independently refined molecules, i.e., 4592 non-hydrogen atoms, and 55 well-defined water molecules (a preliminary set of coordinates was deposited with the Protein Data Bank, accession code 1THT). There are two fragments in each molecule for which no interpretable electron density is observed. They are five N-terminal residues and a surface loop containing residues 72–83. One other surface loop, residues 168–171, appears to be partly disordered, and its stereochemistry is uncertain. These features are found in each of the two independently refined molecules in the asymmetric unit of the crystal, indicating genuine intrinsic mobility of these fragments. The crystallographic refinement was terminated when no further improvement could be achieved in the conventional crystallographic *R*-factor value (22% for all data between 8.0 and 2.06 Å), without compromising the stereochemistry of the model. The root-mean-square (rms) deviation from ideality for bond lengths in the current model is 0.013 Å and for planar bond angles is 2.94°. The real space correlation factor (Jones *et al.*, 1991) shows little variation with sequence in both molecules, and its average value is approximately 0.8. The only areas where it is significantly lower are the above mentioned loops containing residues 72–83 and 168–171. An analysis of the secondary structure using PROCHECK (Laskowski *et al.*, 1992) shows that all non-glycine amino acids well-defined in the electron density map fall within the most favored regions (89.6%) and additional allowed regions (9.8%) of the Ramachandran plot. A notable exception is the catalytic Ser114 whose secondary structure—addressed in detail below—conforms to that of other nucleophiles in the $\alpha/\beta$ hydrolase family (Derewenda & Derewenda, 1992; Ollis *et al.*, 1992). A representative difference electron density is shown in Figure 2.

The tertiary fold of the molecule is remarkably similar to that proposed for the ancestral $\alpha/\beta$ hydrolase (Ollis *et al.*, 1992) (Figure 1a). Particularly striking similarity exists between $C_{14}$ACP-TE and Hal—haloalkane dehalogenase from *Xanthobacter autotrophicus* (Verschueren *et al.*, 1993a,b) (Figure 1b,c). A putative active site was identified from the structure on the carbonyl end of the central $\beta$-sheet, a typical location for $\alpha/\beta$ hydrolases. It is located in a solvent-accessible crevice and contains a typical "catalytic triad" of Ser114 [and not Ser77, as suggested earlier by Ferri and (1991)], His241, and Asp211 (Figure 2). The hydrogen bonds observed within this constellation of amino acids (i.e., SerO$\gamma$H···HisN$\epsilon$2 and HisN$\delta$1···AspO$\delta$1) are structurally analogous to those found

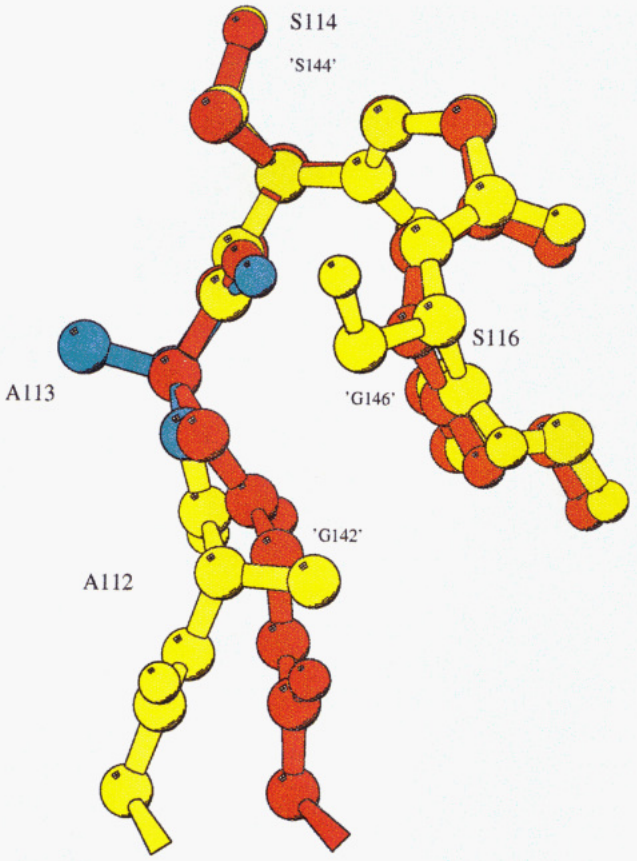


FIGURE 3: Comparison of the stereochemistry of the nucleophilic elbows in the *V. harveyi* thioesterase (yellow) and the *R. miehei* lipase (red). For clarity we show only the key side chains; the smaller numbers relate to the *R. miehei* lipase. The blue amino acid in the $C_{14}$ACP-TE structure, Ala113 (the side chain of the analogous His143 from the *R. miehei* lipase is not shown), is the one whose altered secondary structure is responsible for the "opening" of the elbow, accommodating amino acids other than Gly in positions 1 and 5 (see text for details). The figure was generated by MOLSCRIPT (Kraulis, 1991). The coordinates of the *R. miehei* lipase are those found in the 3TGL entry in the Protein Data Bank.

in other serine hydrolases. However, the "handedness" of the triad is opposite to that found in serine proteinases and identical to that seen in lipases and acetylcholinesterase (Figure 2). Ser114 was found to be within a structural context analogous to the so-called nucleophilic elbow (Ollis *et al.*, 1992), i.e., at the center of a sharp $\gamma$-turn between a $\beta$-strand and an $\alpha$-helix, and shows a strained secondary conformation ($\phi = 53°$, $\psi = -127°$), a hallmark of the nucleophile in the $\alpha/\beta$ hydrolase superfamily (Derewenda & Derewenda, 1991; Ollis *et al.*, 1992). Unexpectedly, the amino acid sequence within this turn (Ala-Ala-Ser-Leu-Ser) shows no similarity with the lipase/esterase consensus Gly-X-Ser-X-Gly motif (Brenner, 1988).

The discrepancy between the biochemical data—implicating Ser77 in catalysis—and the crystal structure prompted us to reexamine earlier results of mutagenesis. Two mutants were characterized by radiolabeling: Ser77 → Gly and Ser114 → Gly. Their ability to form acyl-enzyme intermediates was assessed by labeling them with [$^3$H]myristoyl-CoA using both low and high concentrations of the latter reagent. In *E. coli* extracts the wild-type enzyme was readily labeled using 1 $\mu$M [$^3$H]myristoyl-CoA, as opposed to either of the two mutants. However, when a 10-fold excess of the acylating agent was used, a low level of radioactive labeling in the Ser77 → Gly mutant was observed, while the Ser114 → Gly mutant was inactive. The crystal structure of this mutant showed no differences compared to the wild-type enzyme; in both, the loop containing the amino acid in position 77 is disordered.

As in other $\alpha/\beta$ hydrolases, the main-chain amide on the carboxyl side of the nucleophilic Ser (in this case Leu115) is positioned ideally to serve as one of the two hydrogen bond donors usually found to form the electrophilic oxyanion hole, the purpose of which is to stabilize the tetrahedral intermediates. However, in the present structure we did not find any suitably positioned candidates for the second H-bond donor.

## DISCUSSION

The *V. harveyi* $C_{14}$ACP-TE is the first crystallographically characterized thioesterase. It demonstrates that the enzymatic hydrolysis of the thioester bond proceeds using the same basic catalytic machinery, i.e., a nucleophilic triad of Ser, His, and Asp, as originally found 25 years ago in proteinases (Blow *et al.*, 1969) and subsequently discovered in lipases and oxyesterases.

Equally important is the observation that $C_{14}$ACP-TE is the 13th structurally characterized representative of the $\alpha/\beta$ hydrolase superfamily. The other members are: Hal (Verschueren *et al.*, 1993a,b), dienelactone hydrolase (Pathak & Ollis, 1990), four lipases from the *Rhizomucor miehei* (Brady *et al.*, 1990; Derewenda, Z. S., *et al.*, 1992; Derewenda *et al.*, 1994a,b) and two from the *Geotrichum candidum* families (Schrag *et al.*, 1991; Schrag & Cygler, 1993; Grochulski *et al.*, 1993) of filamentous fungi, the *Pseudomonas glumae* lipase (Noble *et al.*, 1993), human pancreatic lipase (Winkler *et al.*, 1990), acetylcholinesterase (Sussman *et al.*, 1991), cutinase (Martinez *et al.*, 1992), and wheat serine carboxypeptidase II (Liao *et al.*, 1992). The $\alpha/\beta$ hydrolase family thus constitutes the second largest family of structurally related enzymes, after the TIM barrel (or $\alpha_8/\beta_8$ barrel) family. One of the intriguing questions raised by the discovery of the $\alpha/\beta$ fold is its evolutionary origin. The family is made up of several clearly homologous groups [e.g., the lipases from the *R. miehei* family of filamentous fungi (Derewenda *et al.*, 1994a,b)] but contains also enzymes whose amino acid sequences are unique, e.g., Hal (Verschueren *et al.*, 1993). In this context the structure of $C_{14}$ACP-TE may shed new light on the evolution and function of $\alpha/\beta$ hydrolases. Since FAS is one of the oldest and most conserved enzymatic complexes (fatty acids are essential for all living organisms), it is possible that $\alpha/\beta$ hydrolases evolved as a result of gene duplication of an ancestral fatty acid chain-terminating TE. The similarity between $C_{14}$-ACP-TE and Hal shows that evolution may proceed largely by mutations inserting loops, caps, and lids, modifying substrate specificity, or activation properties.

One of the most conserved features of the $\alpha/\beta$ hydrolase family is the nucleophilic elbow (Ollis *et al.*, 1992; Derewenda & Derewenda, 1991), which is made up of a $\beta$-strand, typically the fifth one in the central sheet, a sharp $\gamma$-turn containing the nucleophile, and an $\alpha$-helix. In a majority of cases, with the exception of Hal, the $\gamma$-turn conforms to the frequently invoked Gly-X-Ser-X-Gly lipase/esterase consensus sequence (Brenner, 1988). It has been argued that the presence of the two glycines in this motif is enforced by the unique secondary structure of the $\gamma$-turn (Derewenda & Derewenda, 1991; Ollis *et al.*, 1992), which brings the $\alpha$-carbons of the residues in positions 1 and 5 within the turn into such close proximity that no side chains can be accommodated in those positions. Contrary to this, in the *V. harveyi* $C_{14}$ACP-TE these positions are occupied by an Ala and a Ser, respectively. The potential steric hindrance is relieved by a change in only one main-

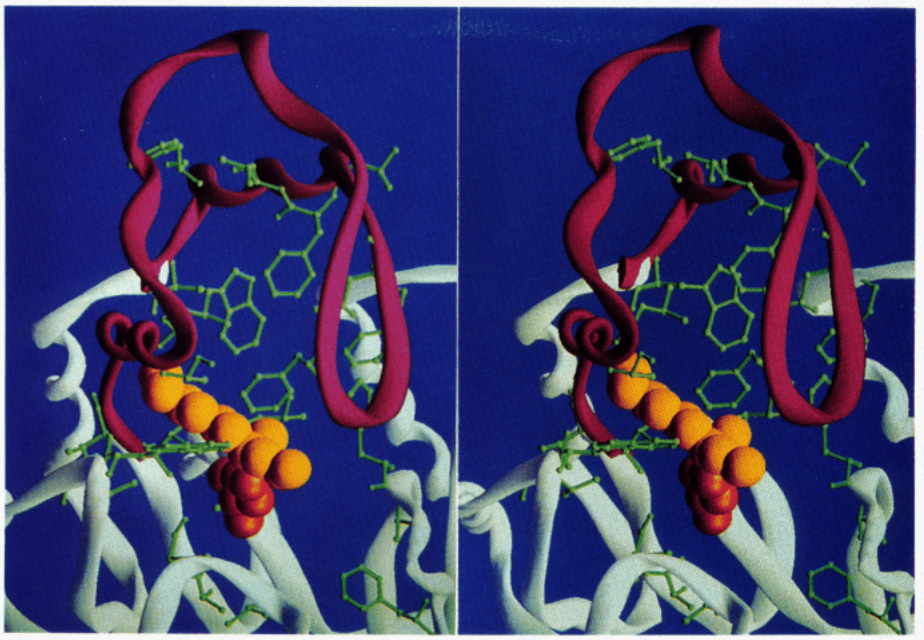

FIGURE 4: Model of the acyl-enzyme intermediate (in stereo) inferred from the crystallographic structure of the native enzyme and the structure of the *R. miehei* lipase complexed with *n*-hexylphosphonate ethyl ester (Brzozowski *et al.*, 1991). The position of the *n*-hexyl moiety is based on the superposition of the catalytic triads in both enzymes. The hydrophobic amino acids which are located in the proximity of the putative acyl binding site are shown in full. Their hydrophobic character is conserved among the four known homologous sequences of this enzyme (Ferri & Meighen, 1991). The cap is shown in pink. Although in the present model there are numerous close contacts between the protein and the fatty acyl moiety, they might be avoided with only slight rearrangements in the packing of some of the amino acids within the cap. The figure was generated using RIBBONS (Carson, 1987).

chain dihedral angle, i.e., the $\phi$ angle of Ala113. In the known structures of lipases the analogous angle is always ca. −105°, while in the $C_{14}$ACP-TE it is −131° (Figure 3). Thus, $C_{14}$-ACP-TE represents the first structurally characterized nucleophilic elbow in which both of the "essential" glycines are replaced by larger amino acids, vividly exposing the dangers of overinterpreting rather feeble sequence homologies and in particular the fragility of the lipase/esterase "consensus" sequence Gly-X-Ser-X-Gly.

In an effort to locate the myristoyl binding site of $C_{14}$-ACP-TE, we have superimposed its atomic model on the active center of the *R. miehei* lipase complexed with *n*-hexylphosphonate ethyl ester (Figure 4). The *n*-hexyl moiety, oriented as in the *R. miehei* complex, protrudes into the space between the main domain of the enzyme and the "cap". This putative pocket is lined with a number of amino acids whose hydrophobic character is conserved among the four homologous sequences known for this enzyme (Ferri & Meighen, 1991). Interestingly, in Hal a topologically equivalent cap, also lined internally with hydrophobic residues, interacts with the substrate (Verschueren *et al.*, 1993a,b). These results agree with our hypothesis of divergent evolution of $\alpha/\beta$ hydrolases from ancestral thioesterases.

The solution of the crystal structure of $C_{14}$ACP-TE resulted in a reassessment of the earlier assignment of Ser77 as the nucleophile. Our present mutational and radiolabeling studies confirm that Ser114 is absoluteiy essential for activity, although the Ser77 → Gly mutant was shown to be significantly impaired. The role of His241 in catalysis was also recently confirmed by site-directed mutagenesis studies of a homologous TE from *Photobacterium phosphoreum* (Ferri & Meighen, 1994). It remains puzzling why mutations in a disordered surface loop, quite distant from the active site, should affect the enzyme's catalytic performance. The crystal structure of the Ser77 → Gly mutant shows no structural changes in the protein resulting from the mutation. A possible explanation is that the loop containing Ser77 interacts in some way with the substrate. Efforts are under way to solve the structure of the acyl-enzyme complex.

Finally, we note that we can identify only one of the two expected hydrogen bond donors within the oxyanion hole. Interestingly, in most neutral lipases, the process of interfacial activation involves a conformational change, which apart from making the active center accessible to solvent, completes the formation of the oxyanion hole (Brzozowski *et al.*, 1991; Derewenda, U., *et al.*, 1992; van Tilbeurgh *et al.*, 1993). Lipolytic enzymes not activated at an oil–water interface appear to have a preformed oxyanion hole (Martinez *et al.*, 1994). We find that, in the $C_{14}$ACP-TE, a highly mobile loop comprising residues 168–171 is located in the immediate proximity of the substrate binding site, and one of its main-chain amides could assume a favorable position to act as an H-bond donor in the oxyanion hole, with relatively small structural rearrangements. This is very reminiscent of the mechanism by which the main-chain amide of Phe77 in human pancreatic lipase is suitably oriented within the oxyanion hole only after the enzyme undergoes activation (van Tilbeurgh *et al.*, 1993). It is tempting to speculate that interfacial activation in lipases may have its evolutionary roots in the substrate recognition phenomenon of acyl-specific thioesterases.

## ACKNOWLEDGMENT

We thank Dr. G. G. Dodson, University of York, York, U.K., for the use of the laboratory facilities. Z.S.D. acknowledges inspiring discussions with Dr. B. Dijkstra regarding the evolutionary relationships between $\alpha/\beta$ hydrolases. Drs. B. D. Sykes and C. M. Kay (MRC Group in Protein Structure and Function, University of Alberta) are thanked for critical reading of the manuscript.

## SUPPLEMENTARY MATERIAL AVAILABLE

Photograph of the SDS gel electrophoresis of extracts of *E. coli* cells containing wild-type and mutant (Ser77 → Gly,

Ser114 → Gly) luxD genes after reaction with [$^3$H]myristoyl-CoA (1 page). Ordering information is given on any current masthead page.

## REFERENCES


Blow, D. M., Birktoft, J. J., & Hartley, B. S. (1969) *Nature 221*, 337–340.

Brady, L., Brzozowski, A. M., Derewenda, Z. S., Dodson, E., Dodson, G., Tolley, S., Turkenburg, J. P., Christiansen, L., Huge-Jensen, B., Norskov, L., Thim, L., & Menge, U. (1990) *Nature 343*, 767–770.

Brenner, S. (1988) *Nature 334*, 528–530.

Brunger, A. T. (1988) *X-PLOR Manual*, Yale University, New Haven, CT.

Brzozowski, A. M., Derewenda, U., Derewenda, Z. S., Dodson, G. G., Lawson, D. L., Turkenburg, J. P., Bjorkling, F., Huge-Jensen, B., Patkar, S. A., & Thim, L. (1991) *Nature 351*, 491–494.

Camp, L. A., & Hofmann, S. L. (1993) *J. Biol. Chem. 268*, 22566–22574.

Carey, L., Rodringuez, A., & Meighen, E. (1984) *J. Biol. Chem. 259*, 10216–10221.

Carson, M. (1987) *J. Mol. Graphics 5*, 103–106.

De Renobales, M., Rogers, L., & Kolattukudy, P. (1980) *Arch. Biochem. Biophys. 205*, 464–477.

Derewenda, U., Brzozowski, A. M., Lawson, D. M., & Derewenda, Z. S. (1992) *Biochemistry 31*, 1532–1541.

Derewenda, U., Swenson, L., Green, R., Wei, Y., Dodson, G. G., Yamaguchi, S., Haas, M. J., & Derewenda, Z. S. (1994a) *Nature, Struct. Biol. 1*, 36–47.

Derewenda, U., Swenson, L., Wei, Y., Green, R., Kobos, P. M., Joerger, R., Haas, M. J., & Derewenda, Z. S. (1994b) *J. Lipid Res. 35*, 524–534.

Derewenda, Z. S., & Derewenda, U. (1991) *Biochem. Cell Biol. 69*, 842–851.

Derewenda, Z. S., Derewenda, U., & Dodson, G. G. (1992) *J. Mol. Biol. 227*, 818–839.

Donadio, S., Staver, M. J., McAlpine, J. B., Swanson, S. J., & Katz, L. (1991) *Science 252*, 675–679.

Ferri, S., & Meighen, E. A. (1991) *J. Biol. Chem. 266*, 12852–12857.

Grochulski, P., Li, Y., Schrag, J. D., Bouthillier, F., Smith, P., Harrison, D., Rubin, B., & Cygler, M. (1993) *J. Biol. Chem. 268*, 12843–12847.

Howard, A. J., Gilliland, G. L., Finzel, B. C., Poulos, T. L., Ohlendorf, D. H., & Salleme, F. (1987) *J. Appl. Crystallogr. 20*, 383–387.

Jones, T. A., Zou, J.-Y., Cowan, S. W., & Kjeldgaard, M. (1991) *Acta Crystallogr. A47*, 110–119 .

Kabsch, W. (1987) *J. Appl. Crystallogr. 21*, 916–924.

Kabsch, W., & Sander, C. (1983) *Biopolymers 22*, 2577–2737.

Kratzschmar, J., Krauze, M., & Marahiel, M. A. (1989) *J. Bacteriol. 171*, 5422–5429.

Kraulis, P. J. (1991) *J. Appl. Crystallogr. 24*, 946–950.

Kunkel, T., Roberts, J., & Zabour, R. (1987) *Methods Enzymol. 154*, 367–382.

Lamzin, V. S., & Wilson, K. S. (1993) *Acta Crystallogr. D49*, 129–147.

Laskowski, R. A., MacArthur, M. W., Moss, D. S., & Thornton, J. M. (1992) *PROCHECK v.2: a Program to Check the Stereochemical Quality of Protein Structures*, Oxford Molecular Limited, Oxford, England.

Liao, D-I., Breddam, K., Sweet, R. M., Bullock, T., & Remington, S. J. (1992) *Biochemistry 31*, 9796–9812.

Libertini, L., & Smith, S. (1978) *J. Biol. Chem 253*, 1393–1401.

Lin, C. Y., & Smith, S. (1978) *J. Biol. Chem. 253*, 1954–1963.

Martinez, C., De Geus, P., Lauwereys, M., Mathyssens, G., & Cambillau, C. (1992) *Nature 356*, 615–618.

Martinez, C., Nicolas, A., van Tilbeurgh, H., Egloff, M.-P., Cudrey, C., Verger, R., & Cambillau, C. (1994) *Biochemistry 33*, 83–89.

McDaniel, R., Ebert-Khosla, S., Hopwood, D. A., & Khosla, C. (1993) *Science 262*, 1546–1550.

Noble, M. E. M., Cleasby, A., Johnson, L. N., Egmond, M. R., & Frenken, L. G. J. (1993) *FEBS Lett. 331*, 123–128.

Ollis, D. L., Cheah, E., Cygler, M., Dijkstra, B., Frolow, F., Franken, S. M., Harel, M., Remington, S. J., Silman, I., Schrag, J. D., Sussman, J. L., Verschueren, K. H. G., & Goldman, A. (1992) *Protein Eng. 5*, 197–211.

Pathak, D., & Ollis, D. (1990) *J. Mol. Biol. 214*, 497–525.

Raibaud, A., Zalacain, M., Holt, T. G., Tizard, R., & Thompson, C. J. (1991) *J. Bacteriol. 173*, 4454–4463.

Richardson, J. S. (1981) *Adv. Protein Chem. 34*, 167–339.

Sanjanwala, M., Sun, G. Y., & MacQuarrie, R. A. (1987) *Arch. Biochem. Biophys. 258*, 299–306.

Schrag, J. D., & Cygler, M. (1993) *J. Mol. Biol. 230*, 575–591.

Schrag, J. D., Li, Y., Wu, S., & Cygler, M. (1991) *Nature 351*, 761–764.

Shen, B., & Hutchinson, C. R. (1993) *Science 262*, 1535–1540.

Sussman, J. L., Harel, M., Frolow, F., Oefner, C., Goldman, A., Toker, L., & Silman, I. (1991) *Science 253*, 872–879.

Swenson, L., Ferri, S. R., Green, R., Sharp, A. M., Meighen, E. A., & Derewenda, Z. S. (1992) *J. Mol. Biol. 227*, 572–574.

Tabor, S., & Richardson, C. (1985) *Proc. Natl. Acad. Sci. U.S.A. 82*, 1074–1078.

vanTilbeurgh, H., Egloff, M.-P., Martinez, C., Rugani, N., Verger, R., & Cambillau, C. (1993) *Nature 362*, 814–820.

Verschueren, K. H. G., Seljee, F., Rozeboom, H. J., Kalk, K. H., & Dijkstra, B. W. (1993a) *Nature 363*, 693–698.

Verschueren, K. H. G., Franken, S. M., Rozeboom, H. J., Kalk, K. H., & Dijkstra, B. W. (1993b) *J. Mol. Biol. 232*, 856–872.

Voelker, T. A., Norrell, A. C., Anderson, L., Bleibaum, J., Fan, C., Hankins, D. J., Radke, S. E., & Davies, H. M. (1992) *Science 257*, 72–74.

Winkler, F. K., D'Arcy, A., & Hunziker, W. (1990) *Nature 343*, 771–774.

Zhang, K. Y. J. (1993) *Acta Crystallogr. D49*, 213–222.